Pergamon

J. Biomechanics, Vol. 28, No. 7, pp. 779–790, 1995

0021-9290/95 $9.50 + .00

0021-9290(94)00140-5

LIMITATIONS OF THE STANDARD LINEAR SOLID MODEL OF INTERVERTEBRAL DISCS SUBJECT TO PROLONGED LOADING AND LOW-FREQUENCY VIBRATION IN AXIAL COMPRESSION

Siping Li,*† Avinash G. Patwardhan,*‡ Farid M. L. Amirouche,*† Robert Havey* and Kevin P. Meade*§

*Orthopaedic Biomechanics Laboratory Rehabilitation Research and Development Center, VA Hospital, Hines, Illinois; ‡Department of Orthopaedic Surgery, Loyola University Chicago, Maywood, Illinois; †Department of Mechanical Engineering, University of Illinois at Chicago, Chicago, Illinois; and §Mechanical and Aerospace Engineering Department, Illinois Institute of Technology, Chicago, Illinois, U.S.A.

Abstract—The purpose of this study was to answer the following questions: (1) Can the standard linear solid model for viscoelastic material simulate the influence of disc level and degeneration on the ability of a disc to withstand prolonged loading and low-frequency vibration? (2) How well does the SLS model explain the relationship between the ability of a disc to resist prolonged loading and its ability to resist dynamic loads and dissipate energy when subjected to low-frequency vibration? Responses of human thoracic and lumbar discs were measured in axial compression under a constant load, and for cyclic deformations at three frequencies. Parameters of the SLS model for each disc were determined by a least-squares fit to the experimental creep response. The model was subsequently used to predict the disc's response to cyclic deformations. The SLS model was able to qualitatively simulate the effects of disc level and degeneration on the ability of an intervertebral disc to resist both prolonged loading and low-frequency vibration. However, the model underestimated the stress relaxation, dynamic modulus and hysteresis of thoracic and lumbar discs subjected to low-frequency vibration. The SLS model was unable to explain the relationship between the ability of a disc to resist prolonged loading and its ability to resist dynamic loads and dissipate energy when subjected to low-frequency vibration. Although in the lumbar discs the *steady-state* predictions of the SLS model were significantly correlated to the experimental response, the strength of model predictions decreased with increasing frequency, particularly for hysteresis.

Keywords: Spine; Vibration; Intervertebral disc; Creep; Relaxation.

INTRODUCTION

Epidemiological studies indicate significant association of the low-back complaint with seated vibration exposures and, particularly, vehicular vibration (Frymoyer *et al.*, 1983; Kelsey and Hardy, 1975). Wilder *et al.* (1982) noted that low-frequency vibrations (up to 6 Hz), dominant in many different types of vehicles (such as trains, light and heavy trucks, buses, bulldozers, tractors), can place the operators at a high risk of developing spinal disorders. Anderson (1992) found motor coach operators to be at much higher risk than comparable nonoperators (80.5% vs 50.7%) for spinal disorders such as back and neck pain. In addition to vibration exposure, sustained loading caused by prolonged sitting is also identified as a risk factor associated with the low-back pain syndrome (Wilder *et al.*, 1988).

The response of human spine segments to prolonged compressive loading has been studied using the three-parameter standard linear solid (SLS) model for viscoelastic material (Burns *et al.*, 1984; Keller *et al.*, 1987, 1990). The model parameters were derived using a least-squares fit of the model's response to the experimental creep response. The SLS model showed excellent approximation to the experimental creep response of spinal segments with an average relative error in the range 0.5–11% (mean, 2.3%). Keller *et al.* (1987) showed the SLS model parameters were sensitive to the degeneration grade of human lumbar discs.

It is reasonable to expect that the ability of an intervertebral disc to resist dynamic loads and dissipate energy is related to its ability to resist prolonged loads since both responses are influenced by the viscoelastic properties of the disc tissue. However, there are no studies on the ability of the SLS model to explain the relationship between the disc's responses to prolonged loading and low-frequency vibration. The parameters of a model obtained by fiting the model's response to experimental creep data (response to prolonged loading) are subject to errors. The errors in estimated model parameters arise due to two reasons. First, the creep experiment may be terminated prematurely, resulting in an incomplete representation of a phenomenon over a much longer time scale. Second, the estimated parameters are likely to be very sensitive to the goodness of fit due to the exponential

Received in final form 5 September 1994.

Address correspondence to: Avinash G. Patwardhan, Ph.D., Department of Orthopaedic Surgery, Loyola University Chicago, 2160 S. First Avenue, Maywood, IL 60153, U.S.A.

nature of the function approximating the response (Fung, 1981). Errors in estimating model parameters may adversely affect the model's prediction of the disc's response to low-frequency vibration.

The purpose of this study was to answer the following questions: (1) Can the standard linear solid model for viscoelastic material simulate the influence of disc level and degeneration on the ability of a disc to withstand prolonged loading and low-frequency vibration? (2) How well does the SLS model explain the relationship between the ability of a disc to resist prolonged loading and its ability to resist dynamic loads and dissipate energy when subjected to low-frequency vibration? In order to answer these questions, responses of human thoracic and lumbar discs were measured in axial compression under a constant load, and for cyclic deformations at three frequencies. The parameters of the SLS model for each disc were determined by a least-squares fit to the experimental creep response. The model was subsequently used to predict the disc's response to cyclic deformation. The experimental data and model predictions were analyzed as a function of disc level, disc degeneration, and loading frequency. Quantitative comparisons were made of the two responses.

MATERIALS AND METHODS

Four fresh human cadaveric spinal columns were used. The protocol for handling cadaveric material followed the guidelines of the Center for Disease Control and the regulations of the Hines VA Hospital where the experiments were performed. The subjects were males, and ranged in age from 30 to 65 years (mean: 41.8, S.D. 15.8). Causes of death were unrelated to spine pathology or metabolic bone disease. Two thoracic (T5–6 and T9–10) and two lumbar (L1–2 and L3–4) spinal segments were removed from each column. Thus, a total of 16 specimens (four at each level) were used.

The posterior structures and ligaments were removed leaving the vertebral body–disc–vertebral body test units intact. We chose to characterize the response of isolated disc–body units since studies in the literature have shown the disc to be the primary load-bearing component in axial compression (Tencer *et al.*, 1982). Further, Kasra *et al.* (1992) noted that removal of posterior elements including facets did not significantly affect the dynamic stiffness and hysteresis of spinal segments. The specimens were prepared so that the superior and inferior surfaces were parallel to the mid-transverse plane of the disc. Prior to testing, A–P, lateral, and axial radiographs were obtained of each specimen to rule out bony pathology, and were used to measure the disc height and cross-sectional area. These data were used to calculate stresses and strains needed for data analysis.

Creep tests were performed first. The specimen was subjected to a constant axial compressive load, the magnitude of which depended on the specimen level and corresponded to the estimated body weight above the segment calculated according to Ruff (1950). The applied creep loads ranged from 200 N at T5–6 to 450 N at the L3–4 disc level. An axial compressive load was applied by weights placed on the platform attached to a loading rod (Fig. 1). The loading rod was inserted through ceramic linear bearings in the center of the top plate to allow only axial deformation of the specimen. The specimen was placed on an AMTI multicomponent load cell (AMTI Multicomponent Transducers, AMTI Inc., Newton, MA) to monitor the reaction forces and moments. The total load was applied incrementally by adding successive weights. The total time to reach the desired load level averaged 22.9 s (S.D. 7.37) for the lumbar specimens and 7.64 s (S.D. 1.67) for the thoracic specimens. Resultant axial displacement of the superior vertebral body was measured using two Kaman eddy current transducers with resolutions of 1 μm (Model KD-2300–1S, Kaman Instrumentation Corp., Colorado Springs, CO). The total creep period was 1 h. The load was then removed, and the specimen was allowed to recover for 1 h. Creep data were sampled at 10 Hz, filtered, and averaged, so that the final data file contained approximately 360 data points equally spaced over the 1 h creep duration.

Following the creep test, cyclic axial compression tests were performed using the displacement-control mode on an Instron Universal Testing Instrument (Model 1122, Instron Corporation, Canton, MA). The upper cup of the specimen was rigidly attached to the moving cross head of the Instron, thus allowing only axial deformation of the specimen. The specimen was mounted on an AMTI load cell which measured the reaction forces and moments. The specimen was first subjected to an axial compressive preload equal in magnitude to the load used in the creep test to simulate the body weight above the segment. This was accomplished by applying an axial deformation to the specimen until the desired load level was reached. This axial deformation was then superimposed by a cyclic deformation input with a peak-to-peak magnitude of 100 μm. The peak-to-peak cyclic strains averaged 2.7% (S.D. 0.8) and 1.1% (S.D. 0.2) for the thoracic and lumbar specimens, respectively. The peak-to-peak force reached a maximum value of approximately 430 N. These values were within the physiologic range so as not to cause a permanent deformation of the disc tissue. Based on our preliminary studies, the load–unload cycles were repeated 30 times to ensure that the resultant peak-to-peak force had little change (1–2%) for successive cycles. Subsequent analysis of the data confirmed that the computed dynamic stiffness and area of the hysteresis loop changed little during the last three cycles of the test. These tests were performed at 0.01, 0.1 and 1 Hz. The frequencies of 0.1 and 1 Hz were selected to provide data for physiologic strain rates. An additional strain rate corresponding to a frequency of 0.01 Hz was used

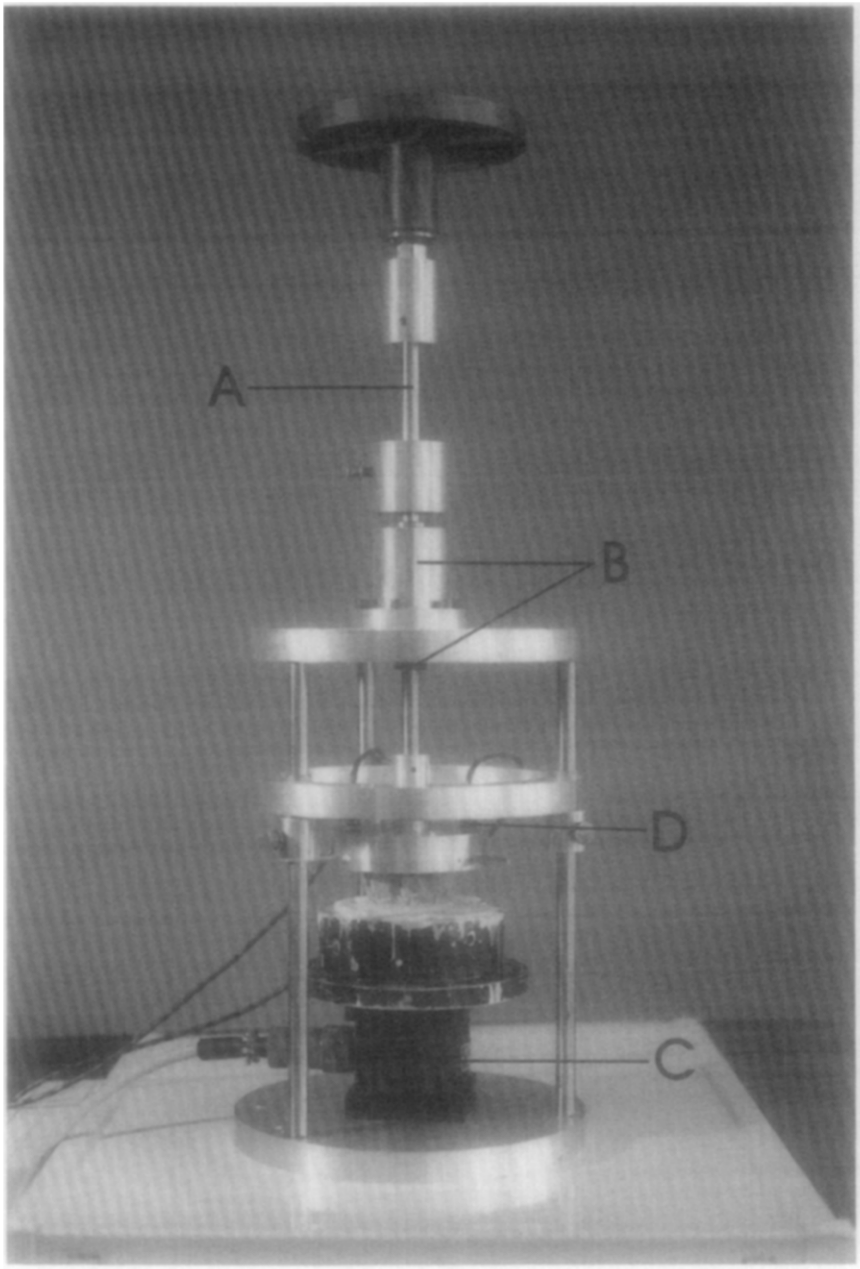

Fig. 1. Apparatus for creep test in axial compression. An axial compressive load was applied by weights placed on the platform attached to a loading rod (A). The loading rod was inserted through ceramic linear bearings (B) in the center of the top plate to allow only axial deformation of the specimen. The specimen was placed on an AMTI multicomponent load cell (C) to monitor the reaction forces and moments acting on the specimen. Resultant axial displacement of the superior vertebral body was measured using two Kaman eddy current transducers (D) with resolutions of 1 μm. The cup holding the superior vertebral body served as the target for the transducers.

to investigate properties over a wider range of strain rates. The load-cell signal and the cross-head motion signal were sampled at 50, 200, and 1500 Hz corresponding to the three frequencies, respectively. A time interval of at least 30 min was allowed between successive tests at different frequencies.

In all creep tests, maximum anterior–posterior and medial–lateral shear forces were less than 5% (means: 2.3% and 2.4%) of the axial compressive force. The maximum reaction moment (flexion-extension or side bending) at the disc center averaged 0.33 Nm, while the maximum axial torque was less than 0.01 Nm. In all cyclic tests, the magnitudes of peak anterior–posterior and medial–lateral shear forces were less than 3% (means: 0.72% and 0.89%) of the peak axial compressive force. The maximum reaction moment (flexion-extension, side bending and axial torque) at the disc center during the cyclic tests averaged 0.13 Nm. The small magnitudes of the A–P and lateral reaction forces and moments at the disc center during creep and cyclic tests indicate that although the specimen was constrained in the vertical direction, the measured response of the specimen can be attributed primarily to axial load.

The total test duration (including creep and cyclic testing) for each specimen was approximately 4–5 h. All experiments were performed at room temperature, and the specimen was kept moist during preparation and testing by loosely wrapping it in saline soaked gauze.

Following testing, the disc was sectioned transversely and the degree of disc degeneration was quantified on an integer scale from 1 to 4 as described by Nachemson (1960). Grade 1 discs showed no macroscopic signs of degeneration in the nucleus and annulus, while grade 4 discs were severely degenerated. Grading of discs was performed by two spine surgeons without *a priori* knowledge of specimen age, sex, and disc level. Each surgeon graded the discs three times in random order. The grading of discs performed by the two surgeons showed strong intra-observer and inter-observer consistency (Li, 1994). An average disc grade for each specimen was obtained by combining the results of the two surgeons. The calculated average value of disc grade was rounded off to the nearest integer value. Nine specimens were classified as having grade 2 disc degeneration, one as grade 3, and six as grade 4. In the following analysis we have defined only two degrees of disc degeneration: mild (grade 2) and moderate–severe (grades 3 and 4). Six of the eight thoracic discs showed mild degeneration, while the remaining two had moderate–severe degeneration. Three of the eight lumbar discs were mildly degenerated, while the remaining five showed moderate–severe degeneration.

Data from creep tests were analyzed as follows. The static stiffness (MN/m) of the disc specimen was calculated as applied creep load divided by the instantaneous axial deformation. The load was divided by the initial disc area to obtain the applied stress, and the axial deformation was divided by the initial disc height to calculate the strain (Keller *et al.*, 1987). The stress–strain data were subsequently used to obtain the parameters of the SLS model used to simulate the creep response of the disc.

Data from the cyclic tests were used to calculate the dynamic stiffness, modulus, and hysteresis. The dynamic stiffness (MN/m) at a loading frequency was calculated by dividing the peak-to-peak load by the input peak-to-peak deformation (100 μm) (Kasra *et al.*, 1992). The dynamic modulus (MPa) was calculated by dividing peak-to-peak stress (peak-to-peak load/initial disc area) by the peak-to-peak strain (100 μm/initial disc height). The area defined by the envelope of the loading and unloading paths represents the energy dissipation during one load–unload cycle. The ratio of the area of the envelope to the area under the loading path was defined as hysteresis (Kasra *et al.*, 1992). For each specimen, the values of dynamic stiffness, modulus, and hysteresis were calculated for the last three cycles of the test and averaged.

A three-parameter (E_1, E_2, and μ) SLS model was used to simulate the creep response of the intervertebral disc. The SLS model is governed by the following differential equation (Flügge, 1975):

$$\sigma + p_1\dot{\sigma} = q_0\varepsilon + q_1\dot{\varepsilon},$$

where σ and ε denote stress and strain, the dot denotes rate of change with respect to time, and

$$p_1 = \frac{\mu}{E_1 + E_2}, \quad q_0 = \frac{E_1 E_2}{E_1 + E_2}, \quad q_1 = \frac{E_2 \mu}{E_1 + E_2}.$$

Simulation of the creep test was done by applying a single-step load input to the SLS model. Although the load in experimental creep tests was applied in multiple steps, this was accomplished within a relatively short period of time ranging from a mean of 7.64 s for thoracic to 22.9 s for lumbar discs (less than 1% of the total creep period of 1 h). Therefore, the single-step load function used in the model development was a reasonable mathematical approximation of the actual loading process. For a given stress step input of magnitude σ_0, the creep response is

$$\varepsilon = \sigma_0\left[\frac{E_1 + E_2}{E_1 E_2} - \frac{1}{E_1}\exp\left(-\frac{E_1}{\mu}t\right)\right]. \quad (1)$$

The constants of the SLS model for each specimen were determined by minimizing the sum of the squared error between the predicted strain and the observed strain during the creep test:

$$\mathrm{Min} f = \sum_i^n (\varepsilon_i^e - \varepsilon_i^p)^2, \quad (2)$$

where ε_i^e is the observed strain at a given time, ε_i^p is the predicted strain (equation (1)) at a given time and n is the number of points in the final data file.

The convergence criterion was for all parameters to be within a relative tolerance of 10^{-6} between two consecutive iterations (Keller *et al.*, 1987). Although a systematic study of the convergence criterion was not performed, we noted that a criterion based on the relative tolerance of 10^{-4} yielded the same results. However, we elected to follow the criterion suggested by Keller *et al.* (1987) to maintain consistency with the previous studies.

The goodness of fit of the model response (equation (1)) to the experimental creep data was expressed in terms of the following error measures:

$$\text{Maximum relative error} = \operatorname*{Max}_{i} \left| \frac{\varepsilon_i^e - \varepsilon_i^p}{\varepsilon_i^e} \right| \tag{3a}$$

and

$$\text{Average relative error} = \frac{1}{n} \sum_{i}^{n} \left| \frac{\varepsilon_i^e - \varepsilon_i^p}{\varepsilon_i^e} \right|. \tag{3b}$$

The model parameters obtained from the creep data were subsequently used to predict the model's response to a cyclic displacement input. The input to the specimen during the cyclic test was simulated using the following function of strain:

$$\varepsilon = \varepsilon_0(1 - \cos \omega t) + \varepsilon_1, \tag{4}$$

where ε_1 is the prestrain resulting from the initial deformation applied to the specimen to create the desired preload, ε_0 is equal to one-half the peak-to-peak cyclic strain input superimposed on the prestrain, and $\omega = 2\pi f$, where f is the frequency. This function accurately simulates the input strain profile of the specimen during the cyclic displacement-control test. Given such a strain input, the resulting stress output takes the following form:

$$\sigma = (\sigma_0 - A - C)\exp(-t/p_1) + A \cos \omega t + B \sin \omega t + C, \tag{5}$$

where σ_0 is the initial stress generated by the prestrain (ε_1) applied on specimen, and

$$A = -\varepsilon_0 \frac{q_0 + p_1 q_1 \omega^2}{1 + \omega^2 p_1^2} \quad B = \omega \varepsilon_0 \frac{q_1 - q_0 p_1}{1 + \omega^2 p_1^2},$$

$$C = q_0(\varepsilon_0 + \varepsilon_1).$$

Using equations (4) and (5) hysteresis loops were generated for the last three cycles of the cyclic load–displacement test. The model-predicted values of dynamic modulus and hysteresis were calculated for each cycle using the methods described previously for the analysis of experimental data. Average values were obtained for the last three cycles of the test.

The dynamic modulus and energy dissipation per unit volume for each cycle at *steady-state* can be expressed as

$$K(\omega) = \frac{q_0 + p_1 q_1 \omega^2}{1 + \omega^2 p_1^2} + i\omega \frac{q_1 - q_0 p_1}{1 + \omega^2 p_1^2}, \tag{6}$$

$$W = \pi \varepsilon_0^2 \omega \frac{E_2^2 \mu}{(E_1 + E_2)^2 + \omega^2 \mu^2}. \tag{7}$$

Hysteresis was expressed as the fraction of the input energy dissipated in one cycle.

Experimental data were analyzed as a function of the disc level and the degree of disc degeneration. Data from the two thoracic levels were pooled together, as were the data from the two lumbar levels. Thus, there were eight specimens each in the thoracic and lumbar groups. Two degrees of disc degeneration were used: mild and moderate–severe. Statistical analysis of creep data was performed using a two-way analysis of variance with the level of significance for rejecting the null hypothesis set at the 5% probability level. Unless otherwise noted, the term 'significant' will be used henceforth to indicate statistical significance with $p \leqslant 0.05$. The experimentally measured dynamic stiffness, modulus and hysteresis were analyzed using repeated measures analysis of variance with two grouping factors. The measurements corresponding to the three frequencies were treated as repeated measures.

The capability of the SLS model to predict the magnitudes of dynamic modulus and hysteresis was evaluated using a linear regression analysis (see for example, Kleinbaum *et al.*, 1988). This analysis was performed separately on data from the thoracic and lumbar discs. For a given comparison, the experimental data and corresponding model prediction were treated as dependent and independent variables, respectively. The regression coefficient of the independent variable was normalized and expressed as standardized regression coefficient using the ratio of standard deviations of the independent and dependent variables. The p values indicated whether or not the model predictions were significantly correlated to the respective experimental values. The strengths of these predictive relationships were indicated by the r^2 values. The model predictions of dynamic modulus and hysteresis were calculated for both the 30th cycle and the steady-state response, and were compared with the experimental data for the 30th cycle. The rationale for doing the latter comparison was as follows. While experimentally the dynamic stiffness and area of the hysteresis loop had reached nearly constant values by the 30th cycle, initial analysis showed that model predictions of hysteresis had not. Therefore, we wanted to examine whether the model's steady-state predictions correlated with experimental observations corresponding to the 30th cycle.

In addition to the magnitudes of dynamic modulus and hysteresis, the load relaxation response of the SLS model to simulated cyclic displacement input was compared with experimental data. The amount of load relaxation at the end of the 30th cycle was expressed as a fraction of the initial preload: $(L_0 - L_t)/L_0$, where L_0 is the initial preload and L_t is the load at the end of the 30th cycle. This allowed us to compare the load relaxation behavior of the model and the specimen at approximately 30, 300 and 3000 s time intervals corresponding to the three testing frequencies of 1, 0.1, and 0.01 Hz, respectively.

RESULTS

The parameters of the SLS model simulating the response of an intervertebral disc to prolonged loading (creep) were influenced by the disc level and the degree of degeneration in lumbar discs. The values of E_1 and μ were significantly larger in the lumbar as compared to the thoracic discs, by 43 and 72%, respectively (Table 1). The time constant ($\tau = \mu/E_1$) was significantly smaller in the thoracic as compared to lumbar discs. The time constant decreased with increasing disc degeneration, with this difference being statistically significant for lumbar discs. This indicates that the equilibrium state will be reached faster in thoracic discs as compared to lumbar, and in lumbar discs with moderate–severe disc degeneration as compared to mildly degenerated discs. No significant effects of disc degeneration were noted on model parameters (E_1, E_2, μ, and τ) of thoracic discs.

The model simulated the difference in load relaxation of thoracic and lumbar discs subjected to low-frequency vibration, although the model underestimated the relaxation response of the discs. The load relaxation at the end of the 30th cycle was significantly greater in thoracic as compared to lumbar discs, indicating that thoracic discs relaxed at a faster rate than lumbar discs (Table 2). Thus, the transient response of a disc to low-frequency vibration is consistent with its response to prolonged loading which showed that thoracic discs reached equilibrium at a faster rate than lumbar discs under a constant load. However, the thoracic and lumbar discs showed significantly larger load relaxation as compared to the model (Table 2, Fig. 2). The discrepancy between the experimental and model-predicted load relaxation at the end of the 30th cycle increased significantly with increasing frequency.

The SLS model could simulate the effects of disc level and degeneration on the ability of a disc to resist dynamic loads when subjected to low-frequency vibration. The dynamic stiffness of thoracic discs was significantly larger than that of lumbar discs, al-

Table 1. Material properties of spinal discs predicted by the SLS model. The creep response was a function of disc level, and was affected by the degree of disc degeneration in lumbar discs. The values of E_1 and μ were significantly larger in the lumbar as compared to the thoracic discs. The time constant ($\tau = \mu/E_1$) was significantly smaller in the thoracic as compared to lumbar discs. The time constant decreased with increasing disc degeneration, with this difference being statistically signficant for lumbar discs. No significant effects of disc degeneration were noted on material properties (E_1, E_2, μ, and τ) of thoracic discs

	Degree of disc degeneration	Thoracic Mean (S.D.)	Lumbar Mean (S.D.)
E_1 (MPa)	Combined	5.32 (1.37)	7.62 (2.20)
	Mild	4.85 (1.16)	9.25 (1.61)
	Moderate–severe	6.71 (1.13)	6.63 (1.99)
E_2 (MPa)	Combined	5.40 (1.09)	5.06 (1.96)
	Mild	5.35 (1.24)	6.35 (1.59)
	Moderate–severe	5.56 (0.72)	4.29 (1.86)
μ (GPa s)	Combined	11.4 (2.71)	19.6 (8.42)
	Mild	10.9 (2.60)	27.4 (8.46)
	Moderate–severe	13.2 (3.04)	15.0 (3.97)
Time Constant (τ) (Min)	Combined	36.2 (4.14)	42.1 (7.68)
	Mild	37.4 (4.04)	48.7 (7.06)
	Moderate–severe	32.6 (2.03)	38.1 (5.04)

Table 2. Relaxation of spinal discs during cyclic deformation test. Experimental and model-predicted values of the amount of load relaxation by the end of the 30th cycle are expressed as a fraction of the initial preload: $(L_0 - L_t)/L_0$, where L_0 is the initial preload and L_t is the load at the end of the 30th cycle. Both the experimental results and model predictions showed that load relaxation at the end of the 30th cycle was significantly larger in thoracic as compared to lumbar discs at all three testing frequencies, indicating that thoracic discs relaxed at a faster rate than lumbar discs. The specimen showed significantly larger load relaxation as compared to the model

	Thoracic		Lumbar	
	Experiment	Model	Experiment	Model
1 Hz	0.31 (0.10)	0.02 (0.00)	0.10 (0.04)	0.01 (0.00)
0.1 Hz	0.47 (0.10)	0.16 (0.02)	0.19 (0.05)	0.08 (0.02)
0.01 Hz	0.83 (0.13)	0.63 (0.08)	0.51 (0.07)	0.40 (0.07)

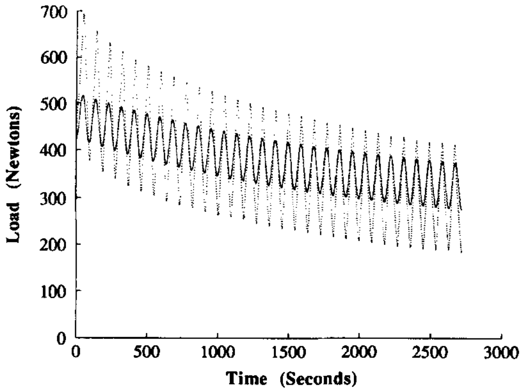

Fig. 2. A comparison of experimental data for a lumbar disc with the response of the SLS model to cyclic deformation input. The load response predicted by the model (solid line) differed from that of the specimen (dotted line). The specimen showed significantly larger load relaxation as compared to the model. The peak-to-peak loads predicted by the model were significantly smaller than those observed experimentally, indicating underestimation of the dynamic modulus by the SLS model.

though the dynamic moduli of thoracic and lumbar discs were similar. These trends in the predicted responses agree with experimental observations (Table 3). Significant effect of disc degeneration was found only on the dynamic modulus. The model predicted the dynamic modulus of lumbar discs to decrease by about 30% with increasing degeneration, which compared favorably with the 38–40% decrease measured experimentally.

However, the model underestimated both the dynamic modulus and hysteresis of thoracic and lumbar discs. The dynamic modulus calculated for the 30th cycle by the SLS model had reached nearly constant (steady-state) value, and ranged from 5.0–5.4 MPa as compared to the experimental values of 10.5–15.5 MPa. The hysteresis values predicted by the model ranged from 0.1% (at 1 Hz) to 3.3% (at 0.01 Hz), while the experimental values were in the 8–16% range. The model predictions of hysteresis in the 30th cycle had not reached steady-state values, and did not correlate with experimental data for both thoracic and lumbar discs ($r^2 < 0.2$, $p > 0.3$).

The steady-state values of dynamic modulus and hysteresis predicted by the SLS model were significantly correlated to experimentally measured values for the lumbar discs, however, the strength of model predictions was modest and decreased with increasing frequency. The steady-state model predictions explained 65–78% and 48–72% of the variation in the experimentally measured modulus and hysteresis, respectively. The strength of the predictive relationships decreased with increasing frequency as indicated by the decreasing r^2 values, particularly for hysteresis (Table 4). The model predicted the hysteresis to decrease significantly with increasing frequency, but the experimental data did not indicate any dependence on frequency.

For the thoracic discs, the steady-state values of dynamic modulus and hysteresis predicted by the SLS model did not correlate with the corresponding experimental data ($p > 0.05$ and poor r^2 values). The steady-state model-predictions explained only 1–7% and 3–43% of the variation in the experimentally measured modulus and hysteresis, respectively (Table 4).

DISCUSSION

Exposure of the spine to low-frequency vibration and to prolonged loading are two important risk factors associated with the low-back pain syndrome. When prolonged loading is combined with low-frequency vibration, e.g. in operating a motor vehicle, the incidence of low-back complaints is significantly increased. Models of the spine can be used to systematically evaluate the combined effects of prolonged loading and low-frequency vibration on the segmental loads and motions in order to help identify potentially harmful working environments and suggest ways to minimize the detrimental effects to the spine. Studies in the literature have proposed a three-parameter SLS model to simulate the creep (prolonged loading) response of a spinal segment. The purpose of this study

Table 3. Mean (S.D.) values of dynamic stiffness (MN/m), modulus (MPa), and hysteresis of spinal discs. The experimentally measured dynamic stiffness was a function of disc level and frequency, and decreased with degeneration in the lumbar discs. At a given frequency, the dynamic stiffness of thoracic discs was significantly larger than that of lumbar discs, although the dynamic moduli of thoracic and lumbar discs were similar. Both the dynamic stiffness and modulus increased significantly when loading frequency was increased from 0.01 to 0.1 Hz, and remained nearly constant thereafter. Effect of disc degeneration was significant only in the lumbar discs. The dynamic modulus of lumbar discs decreased by 38–40% with increasing disc degeneration. Lumbar discs displayed significantly smaller hysteresis than thoracic discs. No clear trends were found for the effects of frequency and disc degeneration on hysteresis

Frequency (Hz)	Thoracic			Lumbar		
	Stiffness	Modulus	Hysteresis	Stiffness	Modulus	Hysteresis
0.01	2.44 (0.60)	10.6 (3.39)	0.16 (0.04)	1.62 (0.31)	10.5 (3.80)	0.08 (0.05)
0.10	3.34 (0.63)	14.4 (3.99)	0.12 (0.02)	2.23 (0.45)	14.3 (5.03)	0.08 (0.04)
1.00	3.73 (0.84)	15.4 (4.83)	0.15 (0.05)	2.42 (0.51)	15.5 (5.47)	0.11 (0.05)

Table 4. Results of linear regression analysis of experimental data and *steady-state* values predicted by the SLS model. Standardized regression coefficients of independent variables (model predictions) are shown along with r^2 and p values. For the lumbar discs, the steady-state model predictions explained 65–78% and 48–72% of the variation in the experimentally measured modulus and hysteresis, respectively. The strength of the predictive relationships decreased with increasing frequency as indicated by the decreasing r^2 values. For thoracic discs, the steady-state model predictions explained only 1–7% and 3–43% of the variation in the experimentally measured modulus and hysteresis, respectively

	Thoracic			Lumbar		
	Std coef	p	r^2	Std coef	p	r^2
Modulus (Hz)						
0.01	0.26	NS	0.07	0.89	S	0.78
0.10	0.14	NS	0.02	0.84	S	0.70
1.00	0.08	NS	0.01	0.81	S	0.65
Hysteresis (Hz)						
0.01	0.65	§	0.43	0.85	S	0.72
0.10	0.17	NS	0.03	0.76	S	0.57
1.00	0.64	†	0.41	0.69	‡	0.48

NS: Not significant; S: Significant ($p < 0.05$); §: $p = 0.08$, †: $p = 0.09$, ‡: $p = 0.06$.

was to investigate whether the SLS model, derived from the creep response, can also simulate the response of the disc to cyclic displacements over a range of physiologic frequencies. The parameters of the SLS model were obtained from a specimen's creep response, and the model's dynamic response was subsequently compared to the experimentally measured response of the same specimen.

One of the limitations of this study is the small sample size within the cells of the two-factor experimental design. This is particularly true in the thoracic spine where only two of the eight specimens were noted to have moderate–severe disc degeneration. Thus, the inability of the study to detect significant effects of degeneration in thoracic discs is associated with low statistical power due to small sample size. A second limitation is related to the load/strain history. Response of viscoelastic materials is known to be affected by load/strain history. In this study each specimen was tested first in creep followed by cyclic testing at three successively increasing frequencies. These tests were not performed in a random order. In order to minimize the effect of load/strain history we allowed a recovery period of 30–60 min between successive tests. Model predictions of a disc's response to cyclic deformation therefore did not take into consideration the effects of load/strain history. Further investigations are needed to delineate the effect of this factor on experimental data and model performance. Finally, it is realized that the inability of the *ex vivo* experimental conditions to fully replicate the *in vivo* physiologic conditions may affect spinal segment responses (Keller *et al.*, 1990). However, this source of error is not likely to substantially influence the results concerning the performance of the model since the data used to derive the model and to evaluate its validity were gathered under the same experimental conditions.

The SLS model was derived based on the creep response of the intervertebral disc. The model was given a step-load input to simulate the loading process in experimental creep tests. However, the load in experimental creep tests was applied in multiple steps, although within a relatively short period of time ranging from a mean of 7.64 s for thoracic to 22.9 s for lumbar discs (less than 1% of the total creep period of 1 h). Therefore, the single-step load function used in the model development was an approximate mathematical representation of the actual loading process. The effect of the single-step function approximation of the actual multiple-step loading process on model development was investigated using data from one thoracic and one lumbar disc. All data from the initial loading period were used and the model was given a multiple-step load input accordingly. The creep response of the model was then used in the least-squares fit to obtain the model parameters. Using a single-step load function to simulate the multiple-step loading process caused a difference of less than 5% in model's prediction of dynamic modulus and hysteresis (Li, 1994). This compliments the findings of Haut and Little (1972), who observed that experimental stress relaxation response of collagen fibers was not dependent on the amount of time (up to 23 s) used for reaching a desired level of strain.

The experimental results of this study compare favorably to values reported by previous investigators for static stiffness, dynamic stiffness, and hysteresis of thoracic and lumbar segments (Table 5). Our observations that lumbar discs had significantly smaller dynamic stiffness and hysteresis than thoracic discs agree with the findings reported by Koeller *et al.* (1984). The values of E_1, E_2 and μ of the SLS model are of the same order of magnitude as those reported in the literature (Keller *et al.*, 1987), although the characteristic time constant (μ/E_1) obtained in this study is larger than that found by Keller *et al.* (1987). Fung (1981) suggested that a measured characteristic time of a relaxation experiment can be affected by the length of the experiment. In this study the length of

Table 5. Comparison of experimental results with previous studies. The experimental results of this study compare favorably to values reported by previous investigators for static stiffness, dynamic stiffness, and hysteresis of thoracic and lumbar segments. The values of E_1, E_2 and μ of the SLS model are of the same order of magnitude as those reported in the literature, although the time constant (μ/E_1) obtained in this study is larger possibly due to the longer duration of the creep experiment

Measured quantity	Present study	Previous studies	
Static stiffness (MN/m)			
Thoracic	1.43	1.24	Panjabi *et al.* (1976)
Lumbar	0.83	0.8	Berkson *et al.* (1979) (without posterior elements)
		0.5–0.62	Tencer *et al.* (1982)
		0.4–0.6	Edwards *et al.* (1987)
Dynamic stiffness (MN/m) at 1 Hz			
Thoracic	3.73	3.1†	Koeller *et al.* (1984)
Lumbar	2.42	1.5*	Kasra *et al.* (1992) (without posterior elements)
		1.8†	Koeller *et al.* (1984)
Hysteresis (%) at 1 Hz			
Thoracic	0.15	0.14†	Koeller *et al.* (1984)
Lumbar	0.11	0.11†	Koeller *et al.* (1984)
		0.05*	Kasra *et al.* (1992) (without posterior elements)
Creep response (Lumbar)			
E_1 (MPa)	7.62	6.26	Keller *et al.* (1987)
E_2 (MPa)	5.06	1.61	
μ (GPa s)	19.6	5.41	
τ (μ/E_1, min)	42.1	9.87	

*Value estimated from graphical results. Cyclic load tests with a 400 N preload and approximately 20 N load amplitude.
†Value estimated from graphical results. Cyclic load tests with a 650 N preload and 400 N load amplitude.

the creep experiments was 1 h as compared to 30 min used by Keller *et al.* (1987), and this may be a factor responsible for the discrepancy. The effect of the duration of the creep experiment on the parameters of the SLS model needs to be examined further. The effects of degeneration seen in this study agree with previous reports. With increasing degree of disc degeneration, the values of E_1, μ, and time constant τ decreased significantly in lumbar discs. Similar effects of disc degeneration on creep response have been reported previously (Kazarian, 1975; Keller *et al.*, 1987; Nachemson *et al.*, 1979). Although the specimens tested in the present study did not include posterior bony and soft tissue structures, the compressive response, in general, compared well with that reported for the intact spinal segments. This is consistent with the earlier findings that the disc is the primary load bearing structure in compression.

The parameters of the SLS model obtained using a least-squares fit to the experimental creep response are very sensitive to the goodness of fit. To demonstrate this sensitivity a numerical experiment was performed using data from one of the thoracic specimens. The optimum set of model parameters ($E_1 = 6.39$ MPa, $E_2 = 5.08$ MPa, $\mu = 13.3$ GPa s) obtained using equation (2) resulted in an average relative error of 0.48% between the experimental data and predicted creep response. For the same specimen, another set of model parameters was obtained ($E_1 = 6.80$ MPa, $E_2 = 5.29$ MPa, $\mu = 10.4$ GPa s) by relaxing the convergence criterion. This set of model parameters produced an average relative error of 1.1% between the experimental data and model's creep response. A comparison of the fit of the two model responses to experimental creep data (Fig. 3) demonstrates that substantial differences in the model parameters lead to a small difference in the average relative error (a measure of goodness of fit). Errors in the estimated values of model parameters affect predictions of dynamic modulus and hysteresis. For example, the steady-state values of hysteresis predicted by the two sets of model parameters differ by 32%. Thus, a seemingly small difference in average relative errors (0.48% vs 1.1%) in the least-squares fit of experimental creep response can be associated with substantial differences in predictions of the dynamic response.

The SLS model was better able to simulate the creep response of lumbar discs as compared to thoracic discs. The maximum relative errors for thoracic and lumbar discs were 10.2% (S.D. 1.7) and 6.3% (S.D. 1.7), respectively. The average relative errors for thoracic and lumbar discs were 0.72% (S.D. 0.12) and 0.46% (S.D. 0.11), respectively. Both the maximum and average relative errors were significantly greater in the thoracic discs as compared to lumbar. In the lumbar discs, the steady-state predictions of the SLS model, derived from the creep response, were significantly correlated to experimentally measured response ($p < 0.05$). However, for the thoracic discs the model predictions of modulus and hysteresis correlated poorly with the corresponding experimental

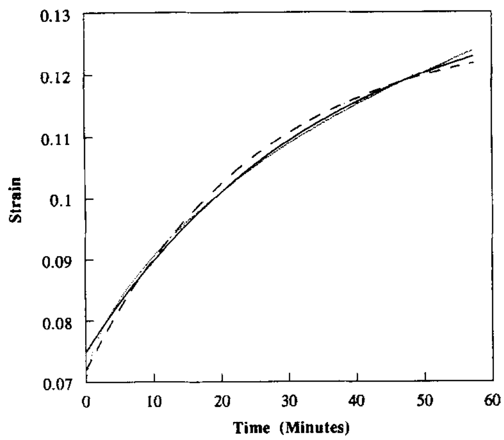

Fig. 3. A comparison of the experimental creep response (dotted line) for a thoracic disc and the response of the SLS model. Two model responses are shown. The optimum set of model parameters ($E_1 = 6.39$ MPa, $E_2 = 5.08$ MPa, $\mu = 13.3$ GPa s) obtained using equation (2) resulted in an average relative error of 0.48% between the experimental data and model's creep response (solid line). For the same specimen, another set of model parameters was obtained ($E_1 = 6.80$ MPa, $E_2 = 5.29$ MPa, $\mu = 10.4$ GPa s) by relaxing the convergence criterion which produced an average relative error of 1.1% between the experimental data and model's creep response (dashed line). This comparison demonstrates that substantial differences in the model parameters lead to a small difference in the average relative error (a measure of goodness of fit).

data ($p > 0.05$ and poor r^2 values). It is possible that significantly larger errors in the least-squares fit of creep response may have introduced larger errors in the estimated model parameters for thoracic discs as compared to lumbar discs. Since predictions of dynamic modulus and hysteresis are affected by parameter values, this may have contributed to the poor predictive performance of the SLS model for thoracic discs. A more thorough sensitivity analysis may reveal the sensitivity of the predicted dynamic response to variations in individual model parameters.

The trends predicted by the SLS model for dynamic modulus and hysteresis as a function of loading frequency did not agree with experimental observations. In particular, the model predicted the hysteresis to decrease significantly with increasing frequency, but the experimental data did not indicate any clear trends. This incompatibility between experimentally observed behavior of hysteresis and that predicted by a model with finite number of springs and dashpots was described previously by Fung (1981).

The SLS model, derived from the creep response (load-control test) has limitations in simulating the stress–relaxation behavior inherent in the disc's response to cyclic deformation (displacement-control test). The discrepancy between the experimental and model-predicted load relaxation at the end of the 30th cycle increases significantly with increasing frequency of cyclic test (Table 2). The differences in the stress–relaxation responses of the model and specimen may be responsible for the lack of correlation between the experimental data and the magnitude of hysteresis predicted by the SLS model for the 30th cycle. It is possible that the dynamic response of the SLS model derived from creep response may correlate better with the response of the disc to cyclic load input, since both the static and cyclic tests are load-control experiments. Conversely, the disc's response to cyclic deformation may be better predicted by a model derived from the stress relaxation response. Further studies are needed to explore this phenomenon.

The standard linear solid (SLS) model for viscoelastic materials was able to qualitatively simulate the effects of disc level and degeneration on the ability of an intervertebral disc to resist both prolonged loading and low-frequency vibration. However, the model underestimated the stress relaxation, dynamic modulus and hysteresis of thoracic and lumbar discs subjected to low-frequency vibration. The SLS model was unable to explain the relationship between the ability of a disc to resist prolonged loading and its ability to resist dynamic loads and dissipate energy when subjected to low-frequency vibration. For the thoracic discs, the model predictions correlated poorly with the corresponding experimental data. In the lumbar discs, the *steady-state* predictions of the SLS model were significantly correlated to the experimental response ($p < 0.05$). However, the strength of model predictions was modest and decreased with increasing frequency, particularly for hysteresis. The model predicted a significant decrease in the ability of the discs to dissipate energy with increasing frequency, but the experimental data did not indicate any dependence on frequency.

Acknowledgments—The study was supported in part by funds from the Hines VA Rehabilitation Research and Development Center and the Department of Orthopaedic Surgery, Loyola University Chicago. Brian Dunlap and John Schaefer of the Hines VA Model Shop fabricated the experimental set-up. Grading of discs was performed by Drs Mark Lorenz and Scott Hodges. Assistance in statistical analysis was provided by Ms Lori Vrbos. Patrick Carrico helped in preparing illustrations. We are grateful to these individuals for their help.

REFERENCES

Anderson, R. (1992) The back pain of bus drivers. Prevalence in an urban area of California. *Spine* **17**, 1481–1488.

Berkson, M. H., Nachemson, A. and Schultz, A. B. (1979) Mechanical properties of human lumbar spine motion segments—Part II. Responses in compression and shear; influence of gross morphology. *J. biomech. Engng* **101**, 53–57.

Burns, M. L., Kaleps, I. and Kazarian, L. E. (1984) Analysis of compressive creep behavior of the intervertebral unit subjected to a uniform axial loading using exact parametric solution equations of Kelvin-solid models—Part I. Human intervertebral joints. *J. Biomechanics* **17**, 113–130.

Edwards, W. T., Hayes, W. C., Posner, I., White, A. A. and Mann, R. W. (1987) Variation of lumbar spine stiffness with load. *J. biomech. Engng* **109**, 35–42.

Flügge, W. (1975) *Viscoelasticity*. Springer, New York.

Frymoyer, J. W., Pope, M. H., Clements, J. H., Wilder, D. G., MacPherson, B. and Ashikaga, T. (1983) Risk factors in low back pain: an epidemiologic survey. *J. Bone Jt Surg.* **65A**, 213–216.

Fung, Y. C. (1981) *Biomechanics. Mechanical Properties of Living Tissue*, pp. 226–237. Springer, New York.

Haut, R. C. and Little, R. W. (1972) A constitutive equation for collagen fibers. *J. Biomechanics* **5**, 423–430.

Kasra, M., Shirazi,-Adl, A. and Grouin, G. (1992) Dynamics of human lumbar intervertebral joints—experimental and finite-element investigations. *Spine* **17**, 93–102.

Kazarian, L. E. (1975) Creep characteristics of the human spinal column. *Orthop. Clin. North Am.* **6**, 3–18.

Keller, T. S., Holm, S. H., Hansson, T. H. and Spengler, D. M. (1990) The dependence of intervertebral disc mechanical properties on physiologic conditions. *Spine* **15**, 751–761.

Keller, T. S., Spengler, D. M. and Hansson, T. S. (1987) Mechanical behavior of the human lumbar spine. I. Creep analysis during static compressive loading. *J. Orthop. Res.* **5**, 467–478.

Kelsey, J. L. and Hardy, R. J. (1975) Driving of motor vehicles as a risk factor for acute herniated lumbar intervertebral disc. *Am. J. Epidemiol.* **102**, 63–73.

Kleinbaum, D. G., Kupper, L. L. and Muller, K. E. (1988) *Applied Regression Analysis and Other Multivariate Methods*. PWS-Kent Publishing Co., Boston.

Koeller, W., Meier, W. and Hartmann, F. (1984) Biomechanical properties of human intervertebral discs subjected to axial dynamic compression—a comparison of lumbar and thoracic discs. *Spine* **9**, 725–733.

Li, S. (1994) Response of human intervertebral discs to prolonged axial loading and low-frequency vibration. Ph.D. Thesis, Department of Mechanical Engineering, University of Illinois at Chicago, Chicago, IL.

Nachemson, A. (1960) Lumbar intradiscal pressure. *Acta orthop. scand.* **43** (Suppl.), 1–104.

Nachemson, A. L., Schultz, A. B. and Berkson, M. H. (1979) Mechanical properties of human lumbar spine motion segments. Influence of age, sex, disc level, and degeneration. *Spine* **4**, 1–8.

Panjabi, M. M., Brand, R. A. and White, A. A. (1976) Three-dimensional flexibility and stiffness properties of the human thoracic spine. *J. Biomechanics* **9**, 185–192.

Ruff, S. (1950) Brief acceleration: less than one second. *German Aviat Med World War II* **1**, 584-597.

Tencer, A. F., Ahmed, A. M. and Burke, D. L. (1982) Some static mechanical properties of the lumbar intervertebral joint, intact and injured. *J. biomech. Engng* **104**, 193–201.

Wilder, D. G., Pope, M. H. and Frymoyer, J. W. (1988) The biomechanics of lumbar disc herniation and the effect of overload and instability. *J. Spinal Disorders* **1**, 16–32.

Wilder, D. G., Woodworth, B. B., Frymoyer, J. W. and Pope, M. H. (1982) Vibration and the human spine. *Spine* **7**, 243–254.